https://doi.org/10.5194/egusphere-2024-1302
Preprint. Discussion started: 21 May 2024

Long-lasting high-latitude volcanic eruptions as a trigger for sudden stratospheric warmings: An idealized model experiment.

Hera Guðlaugsdóttir[1,2], Yannick Peings[2], Davide Zanchettin[3], Gudrun Magnusdottir[2]

[1]University of Iceland, Institute of Earth Sciences, 102 Reykjavík, Iceland

[2]University of California Irvine, Department of Earth System Science, Irvine CA 92697-3100, United States

[3]University Ca'Foscari of Venice, Department of Environmental Sciences, Informatics and Statistics, 30123 Venice, Italy

Correspondence to: Hera Guðlaugsdóttir (hera@hi.is)

Abstract

The temporary enhancement of the stratospheric aerosol layer after major explosive volcanic eruptions can trigger climate anomalies beyond the duration of the radiative forcing. Whereas the mechanisms responsible for long-lasting response to volcanic forcing have been extensively investigated for tropical eruptions, less is known about the dynamical response to high-latitude eruptions. Here we use global climate model simulations of an idealized long-lasting (6 months) northern hemisphere high-latitude eruption to investigate the climate response during the first three post-eruption winters, focusing on the dynamics governing the stratospheric polar vortex. Our results reveal that two competing mechanisms contribute to determining the post-eruption evolution of the polar vortex: 1) A local stratospheric mechanism whereby increased absorption of thermal radiation by the enhanced aerosol layer yields a polar vortex strengthening via a thermal wind response. 2) A bottom-up mechanism whereby surface cooling yields an increase in atmospheric wave activity that propagates into the winter stratosphere, leading to a weakening of the polar vortex, also seen as an increased occurrence of sudden stratospheric warming events (SSWs). The local stratospheric mechanism dominates in the first post-eruption winter, while the bottom-up mechanism dominates in the follow-up winters. The identification of a deterministic response such as increased SSWs following high-latitude volcanic eruptions calls for increased attention to these events as an important source of interannual variability and a possible source of increased seasonal predictability of northern hemisphere regional climates.

https://doi.org/10.5194/egusphere-2024-1302
Preprint. Discussion started: 21 May 2024

1 Introduction

Sulfur-rich volcanic eruptions are an important driver of natural climate variability by imposing short-lived yet possibly very strong radiative anomalies within the atmospheric column. These anomalies occur due to the optical properties of the sulfate aerosols that form when sulfur gasses in the volcanic plume react with water in the atmosphere (Robock, 2000; Timmreck, 2012; Zanchettin, 2017). In general, sulfate aerosols scatter short-wave radiation thereby cooling the surface and absorb long-wave radiation resulting in a warm layer in the stratosphere. This direct radiative effect can alter both meridional surface and stratospheric temperature gradients that can, in turn, initiate further dynamical climate responses on seasonal to decadal time scales (Church et al., 2005; Gleckler et al., 2006; Stenchikov et al., 2009; Shindell et al., 2009; Otterå et al., 2010; Zanchettin et al., 2012; Swingedouw et al., 2015). Over the past decade or so, several studies have shown that high-latitude, Northern Hemisphere (NH) eruptions appear to lead to a different climate response compared to tropical eruptions (Meronen et al., 2012; Pausata et al., 2015; Guðlaugsdóttir et al., 2018; Sjolte et al., 2019). Like tropical eruptions, NH extratropical eruptions can also disturb the meridional temperature gradient, especially considering that *a)* the aerosols tend to stay longer in the polar stratosphere (Graf et al., 1994, 2007) and *b)* the tropopause is lower at higher latitudes than at the equator. Spatiotemporal characteristics of volcanic aerosols from NH extratropical eruptions are also very different when compared to tropical eruptions. Therefore, tropical eruptions are not analogs of NH extratropical eruptions, underlining the need for more studies on the latter to further quantify their potential climate impacts (Zanchettin et al., 2016).
When the meridional stratospheric temperature gradient increases because of warming from volcanic sulfate aerosols originating in the tropics, the stratospheric polar vortex becomes stronger due to thermal wind. Conversely, if the meridional stratospheric temperature gradient decreases because of warming at high latitudes, the result is a weakening of the stratospheric polar vortex (Kodera, 1994; Perlwitz & Graf, 1995; Stenchikov et al., 2002; Bittner et al., 2016). A strengthened stratospheric polar vortex can effect the troposphere as the positive phase of the Northern Annular Mode, while a weaker polar vortex is linked to increased likelihood of sudden stratospheric warming events (SSWs) in the stratosphere and a negative Northern Annular Mode at the surface (Haynes, 2005; Domeisen et al., 2020; Huang et al., 2021; Kolstad et al., 2022, and references therein). Given this top-down mechanism, one expects the results of volcanic eruptions to give tropospheric signatures either in observations or in numerical simulations, but the stratosphere is noisy and tropospheric signatures are weak

https://doi.org/10.5194/egusphere-2024-1302
Preprint. Discussion started: 21 May 2024

(Weierbach et al., 2023; DallaSanta and Polvani, 2023; Kolstad et al., 2022; Azoulay et al., 2021; Polvani et al., 2019; Zanchettin et al., 2022; Toohey et al., 2014). Also, the radiative surface cooling following large volcanic eruptions has been shown to impact large-scale modes of climate variability, such as the El Nino-Southern Oscillation and the Atlantic Multidecadal Variability (e.g., Zanchettin et al., 2012; Pausata et al., 2023; Zhu et al., 2022; Dee et al., 2020; Predybaylo et al., 2020; Pausata et al., 2020; Khodri et al., 2017; Colose et al., 2016), which can in turn affect the stratospheric polar vortex via a bottom-up mechanism (e.g., Graf et al., 2014; Peings and Magnusdottir, 2015; Omrani et al., 2022). Since both mechanisms, i.e., the top-down mechanism triggered by stratospheric heating and the bottom-up mechanism triggered by surface cooling, act together in the real world and, in simulations, under realistic volcanic forcing, idealized model experiments are required to assess their relative contribution to uncertainty in post-eruption regional climate variability (Zanchettin et al., 2016).

Icelandic volcanism has played a role in shaping past NH climate variability and will continue doing so. Two Icelandic eruptions during the past 2000 years, namely Eldgjá in ~939 CE and Laki in 1783 CE, are considered to have had a significant impact even on global climate variability (Brugnatelli and Tibaldi, 2020; Zambri et al., 2019; Oppenheimer et al., 2018; Thordarson and Self, 2003; Stothers, 1998). These types of effusive eruptions are common in Iceland where their duration can extend over years. Eruption history as well as dense monitoring network of Icelandic volcanic systems tell us that many of these systems are currently on the verge of an eruption, having already produced some of the largest volcanic eruptions over the past millennia (e.g., Öræfajökull, Bárðabunga and Hekla, Larsen & Guðmundsson, 2014; Barsotti et al., 2018; Einarsson, 2019). Therefore history and current activity makes these types of eruption an ideal reference case to explore the potential climatic impacts following NH eruptions and to test hypotheses about the underlying mechanisms driving the climate response.

In this study we perform idealized, long-lasting high-latitude volcanic perturbation experiments using The Community Earth System Model version 1 (CESM1) both in coupled and an atmosphere-only mode to assess i) the response within of NH stratospheric polar vortex and ii) the resulting NH tropospheric response during the first three winters following the eruption, referred to as post-eruption winters in the text. This paper is organized in the following manner: Section 2 describes the model, experimental design and diagnostics, results for each winter are presented in section 3, where we end with summarizing discussions in section 4.

https://doi.org/10.5194/egusphere-2024-1302
Preprint. Discussion started: 21 May 2024

2 Methods

2.1. The Global Climate Model

We use the Community Earth System Model (CESM) version 1, from the National Center for Atmospheric Research (NCAR). In our configuration of CESM1, the atmospheric model is the Whole Atmosphere Community Climate Model, version 4 (WACCM4, Marsh et al., 2013). WACCM4 includes 66 vertical levels (up to 5.1×10^{-6} hPa, ∼140 km) and uses CAM4 physics. We use the specified chemistry version of WACCM4 (SC-WACCM4; Smith et al., 2014), which is computationally less expensive to run, but simulates dynamical stratosphere-troposphere coupling and stratospheric variability that is comparable to the interactive chemistry model version. The SC-WACCM4 experiments are run with a horizontal resolution of 1.9◦ latitude by 2.5◦ longitude and include present-day (year 2000) radiative forcing. A repeating 28-month full cycle of the Quasi-biennial Oscillation (QBO) is included in the SC-WACCM4 experiments through nudging of the equatorial stratospheric winds to observed radiosonde data. In the coupled ocean-atmosphere configuration, the ocean component of CESM1 is the Parallel Ocean Program version 2 (POP2). CESM1 also includes the Los Alamos sea ice model (CICE), the Community Land Model version 4 (CLM4) and the River Transport Model (RTM). CLM is run at a horizontal resolution of 1.9°x2.5°, POP2 and CICE are run at nominal 1° resolution with higher resolution near the equator than at the poles. Further details about CESM1 are given in Hurrell et al. (2013).

Simulations run in atmosphere-only mode with prescribed sea surface temperature (SST) and sea ice concentration (SIC) fields are run with SC-WACCM4 in stand-alone mode and are referred to as *atm-only*. The SST and SIC fields are prescribed and fixed to the 1979-2008 monthly climatology of HadISST observations (Rayner et al., 2003). The coupled experiments are henceforth referred to as *cpl*.

2.2. Volcanic Forcing File

We use the Easy Volcanic Aerosol (EVA) forcing generator (Toohey et al., 2016). EVA provides zonally symmetric stratospheric aerosol optical properties as a function of time, latitude, height, and wavelength (see detailed information on the tool in Toohey et al., 2016). EVA has been used to generate volcanic forcing in both idealized volcanic experiments (e.g., Zanchettin et al., 2016) and for paleoclimate simulations (Jungclaus et al., 2017) contributing to the sixth phase of the coupled model intercomparison project.

https://doi.org/10.5194/egusphere-2024-1302
Preprint. Discussion started: 21 May 2024

We use EVA to prescribe the idealized volcanic aerosol loading corresponding in time and magnitude to that of the 1991 Mt. Pinatubo eruption (14.04 Tg SO_2), but at a midlatitude location. Since the model reads the volcanic forcing as aerosol mass (kg/kg), we scale our forcing file by using the standard aerosol mass input file for CAM4 and 5 (see Neely et al., 2016, Table 1) for the same Pinatubo period. A monthly scaling factor was derived from this linear relationship between the aerosol extinction ($1/m^2$) and the aerosol mass (kg/kg) that was used to scale the initial EVA forcing data (Fig. 1).

The aerosol optical properties for an idealized, long-lasting high-latitude NH eruption are obtained with a two-step approach using our newly obtained scaled forcing. First, we move the injection location northwards so that the center of the aerosol mass is at 65° N latitude and spanning 10-28 km in altitude. We then approximate a 6-month long eruption that starts on May 1 by extending in time the highest monthly value in our forcing data so that the decline in aerosol mass begins 6 months after the start of the eruption or on October 1 (see Fig. 1).

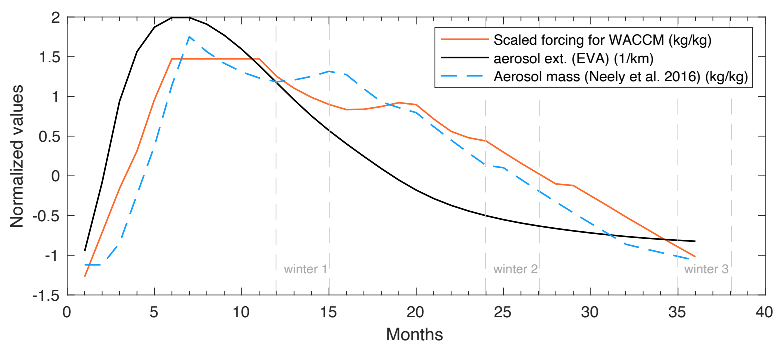

Figure 1: Normalized profiles of the aerosol mass (Neely et al. 2016, blue dashed), aerosol extinction (EVA, black curve) used for the linear scaling method to establish our idealized scaled forcing (red curve) as a function of time (months) from the start of the eruption. Here we assume that the aerosol lifetime at 65° N is the same as at 45° N. Dashed vertical lines show the three winters that we focus on in this study.

2.3. Experimental design

We run two experiments with CESM1. One is with an atmosphere-only version of the model (*atm-only*), the other is with the fully coupled model (*cpl*). In both experiments we run 20 ensemble members using the volcanic forcing and 20 exactly corresponding ensemble members except without the volcanic forcing, which we call the control.

The *atm-only* experiments were run over three full years, which provides two full winters after an eruption is imposed. We found that there was no need to extend the simulations further given the duration of the forcing and short memory of the atmosphere. The *cpl* experiments follow a similar protocol but they were integrated over 15 years to assess the response influenced by oceanic dynamical adjustment. However, in this study we only focus on the first three winters following the eruption. We define the first post-volcanic winter as December of the starting year (year 00) and the following January and February (year 01), the second post-volcanic winter is then December of year 01 and the following January and February of year 02 etc.

Because the QBO is prescribed, and given its important influence on the atmospheric circulation and on the distribution of volcanic aerosols within the stratosphere (Thomas et al., 2009; DallaSanta et al., 2021; Brown et al., 2023), we have been careful to vary the QBO phase that is imposed on the 20 ensemble members. For this, we shift the 28-month QBO cycle by one month for every ensemble member, so that the phasing of the QBO differs from one ensemble member to the next (Elsbury et al., 2021). This avoids potential biases in the climatic response that may be induced by any dominating QBO phase.

2.4. Diagnostics

Model output is analyzed by computing paired anomalies, defined as deviations of each volcanic simulation from the corresponding control simulation (Zanchettin et al., 2022) (volcanic minus control). The statistical significance of the ensemble mean of paired anomalies is assessed at the 95% confidence interval, calculated from all 20 ensemble members, using a two-sided student's t-test.

To identify Sudden Stratospheric Warming (SSW) events we use an algorithm following Charlton and Polvani (2007), where sudden warming events are determined to take place if the 10 hPa zonal-mean zonal wind at 60°N becomes easterly during winter. To evaluate the effects of planetary waves on the zonally averaged stratospheric response, we use the Eliassen Palm flux (EP flux) and its divergence (Edmon et al., 1980). We also use the 3D generalization of the EP flux, the Plumb flux (Plumb, 1985) for a longitudinal representation in the lower troposphere and stratosphere.

3 Results

3.1. Volcanic radiative forcing

https://doi.org/10.5194/egusphere-2024-1302
Preprint. Discussion started: 21 May 2024

Figure 2 shows the net short-wave (SW) flux at the top of the atmosphere for *atm-only* and *cpl* (panels a and b, respectively). The meridional distribution of the mean aerosol mass averaged over the three years is shown in Fig. 2c. The perturbation of solar fluxes is dominated by the obvious strong seasonal evolution, with strong anomalies over the first two post-eruption summers, of similar amplitude despite the already declining forcing in the second post-eruption summer as can be seen in Fig. 1, and substantially smaller anomalies in the third post-eruption summer (Fig. 2a). The solar flux anomalies remain confined north of around 30 °N, with a northward displacement of peak values along the three summers from around 60 °N to around 70° N (Fig. 2a). The maximum value of the aerosol mass center is located between 60 and 70° N as expected, with most of the aerosol mass being located north of 45° N (Fig. 2b). EVA prescribes transport of a small part of the volcanic aerosol to the southern hemisphere, which explains the slight increase between 0 and 60° S. Overall, the radiative forcing thus remains largely confined to NH extratropical summers.

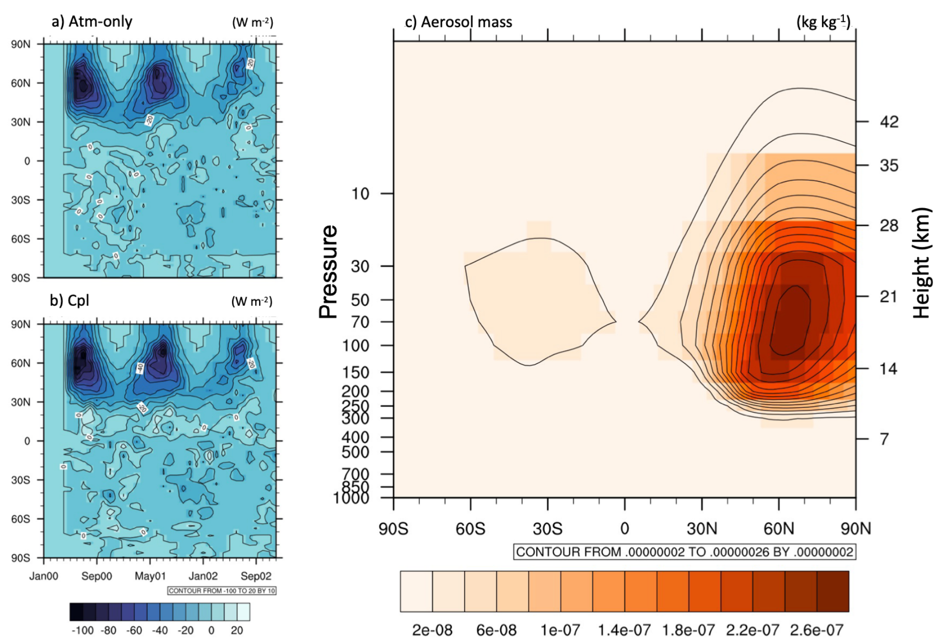

Figure 2: The time evolution of the net solar flux anomaly at the top of the atmosphere at 65° N (contours from -100 to 20 by 10 Wm-2) in a) *atm-only* and b) *cpl*. c) The aerosol mass

https://doi.org/10.5194/egusphere-2024-1302
Preprint. Discussion started: 21 May 2024

averaged over the three years with respect to latitude and pressure height (contours from 2e-8 to 2.6e-7 by 2e-8) in the *atm-only* experiment.

3.2. The Stratospheric response

In addition to cooling due to the negative SW flux anomalies at the top of the atmosphere, stratospheric aerosols absorb longwave (LW) radiation, leading to warming in the lower stratosphere. Accordingly, the strong seasonality in the radiative perturbations described above also characterizes stratospheric temperatures, where a strong increase in the zonally averaged temperature at 50 hPa (T50) is detected north of 30° N during post-eruption summers in both experiments (Fig. 3a and 3b). This summer warming is followed by a net cooling of the polar stratosphere in the first winter seen for both *cpl* and *atm-only*, where the *cpl* reveals intra-seasonal dynamical effects beyond the direct radiative response. A clear difference between *cpl* and *atm-only* is seen in winters 2-3 as captured by T50 (Fig. 3a and 3b) that is also detected in the stratospheric polar vortex index calculated by averaging zonal mean zonal winds at 50 hPa between 70 and 80° N. We will focus on this difference in the following sections.

https://doi.org/10.5194/egusphere-2024-1302
Preprint. Discussion started: 21 May 2024

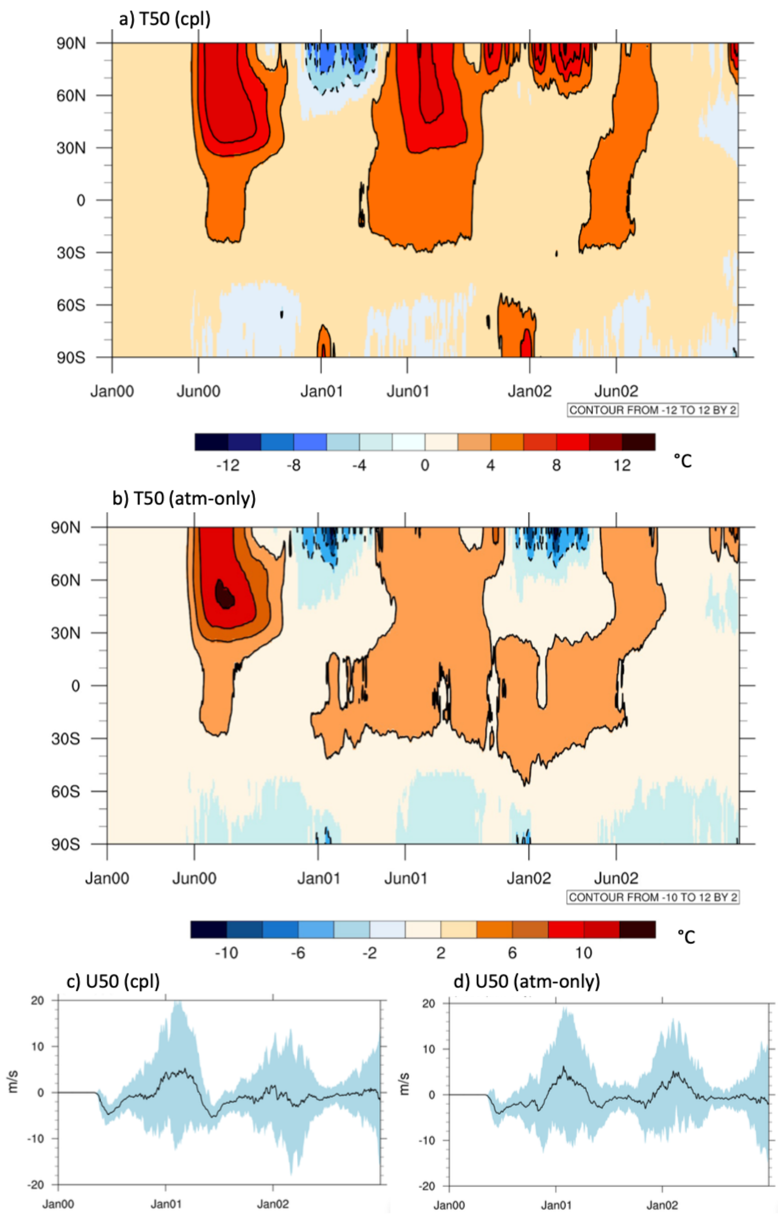

Figure 3. Latitude versus time response of T50 in a) *cpl* and b) *atm-only*. Contours are significant in 95% confidence intervals according to a student's t-test. The stratospheric polar vortex is shown here as the zonal winds at 50 hPa (U50) between 70 and 80° N for c) *cpl* and d) *atm-only* where black lines show ensemble mean and blue shadings show ensemble mean +/- 2 standard deviation.

https://doi.org/10.5194/egusphere-2024-1302
Preprint. Discussion started: 21 May 2024

3.2.1 - First post eruption winter (cpl)

In the first winter of the *cpl* experiment, Fig. 4a depicts the 50 hPa zonal wind and temperature response, showing colder T50 at high latitudes and into midlatitudes over the Atlantic. There is warming over large swaths of the subtropics (to 20° N) and into midlatitudes over the Pacific. The zonal wind at 50 hPa (U50) weakens over the subtropics and into midlatitudes over the Pacific and is stronger in high latitudes and into midlatitudes over the Atlantic. These are signatures of a stronger and colder stratospheric polar vortex. Figure 4d is a meridional cross section showing the response in EP flux and divergence (red contours) in winter 1, along with the winter-mean, zonal-mean jet response (black contours). There is a strong upward EP flux from the surface with convergence of the flux (red dashed contours) in the upper troposphere to lower stratosphere, which weakens the westerlies (black dashed contours). However, the polar vortex itself is reinforced in winter 1, which shows the dominant influence of the local heating due to the volcanic aerosols and the associated increase in the meridional temperature gradient in the stratosphere. This can also be seen in the T50 response in Fig. 3a and Fig. 4a (shading), where a clear dipole of colder temperature at the pole, versus warmer temperature in lower latitudes, is visible. This stratospheric temperature dipole increases the gradient between midlatitudes and the pole, leading to a strengthening of the polar vortex as expected from the thermal wind relationship (as seen from the strengthening of U50 around the pole, Figure 4a, contours).

Figure 4g shows the 850 hPa vertical component of the wave activity flux (the Plumb flux) that allows us to locate sources of wave activity near the surface in winter 1. An upward Plumb flux anomaly is located over the North Pacific Ocean, off the west coast of North America in winter 1. This upward 850 hPa Plumb flux response is also found in the stratosphere (at 150 hPa), although it is located further north (see Supplementary Fig. S1a).

https://doi.org/10.5194/egusphere-2024-1302
Preprint. Discussion started: 21 May 2024

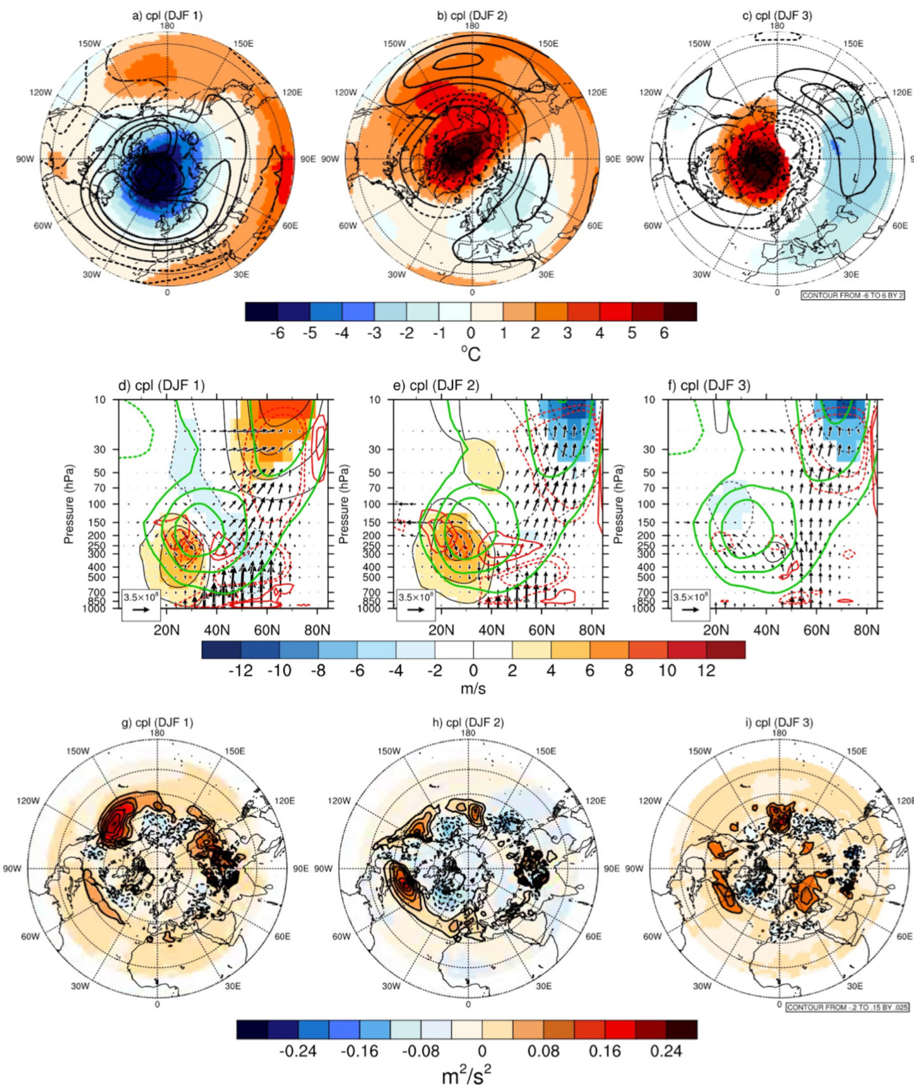

Figure 4: All panels are for the coupled experiment. a-c) Zonal wind (contours) and temperature (shading) response at 50 hPa for winters 1-3, respectively. d-f) EP flux (arrows) and divergence (red contours) response, along with zonal-mean, zonal wind response (black contours) and climatology (green contours) in winters 1-3, respectively. g-i) Vertical component of the Plumb flux response at 850 hPa for winters 1-3, respectively. Contours and color-shaded areas indicate 95% significance according to a student's t-test.

https://doi.org/10.5194/egusphere-2024-1302
Preprint. Discussion started: 21 May 2024

3.2.2. Second post-eruption winter (cpl)

In the second winter, a different pattern emerges as seen in Fig. 4b with strong warming over the polar stratosphere and weaker warming over N America and the Pacific, along with a weakening of U50 at high latitudes with a polar vortex shifted towards Eurasia. An upward propagation of planetary waves persists as seen in Fig. 4e, with a more robust upward EP flux in the lower to mid stratosphere than in winter 1. The direct thermal forcing is therefore the response, and the upward EP flux and its convergence in the stratosphere now weakens the polar vortex as seen in Fig. 4e (black dashed contours). Furthermore, the polar vortex is now more confined over the pole, but as it is slightly shifted toward Eurasia we do not see a clear weakening in the U50 index in Fig. 3c defined over 70-80° N.

In winter 2, the vertical Plumb flux at 850 hPa has decreased in the North Pacific but increased over the North Atlantic and Siberia, pointing to a possible influence of the change in land-sea thermal contrast (Fig. 4h). A significant downward Plumb flux is also occurring in the lower stratosphere over a large area south of 45° N while an upward Plumb flux is seen in the ocean region between the east coast of North America and Southern Europe, forming a dipole pattern in the wave flux in the mid-Atlantic region (Supplementary Fig. S1b).

3.2.3. Third post-eruption winter (cpl)

As can be seen in Fig. 4c, the response in winter 3 is similar to that in winter 2 except that the T50 warming is now confined over the polar stratosphere. An upward propagation of planetary waves continues to persist (Fig. 4f) with an upward pointing wave-activity flux now dominating both at 850 (seen in Fig. 4i) and 150 hPa (Fig. S1.c) where it encircles the polar stratosphere north of 60° N. This polar stratospheric warming that is associated with weaker zonal winds identified in winter 2 and 3 (Fig. 4b and 4c, respectively) is reminiscent of increased SSWs that we now examine using the method of Charlton and Polvani (2007) for these winters. Results from the SSW analysis are presented in Fig. 5, where no significant increase in SSWs is detected in winters 1 and 2. In winter 2, the number of SSW events do increase in the forced experiment (*cpl)* (light-gray bars, 17 events in total) compared to the control (dark-gray bars, 11 events in total) although this difference does not emerge as statistically significant (p-value = 0.11). This changes in winter 3 when the difference between perturbed and unperturbed experiment becomes statistically significant, with 27 SSWs occurring in our forced experiment compared to only 6 in the control experiment (p-value = 2.6e-4). This increase in SSW events agrees well with the U50 and T50 anomalies of winter 3 (Fig. 4c). During winter 2, the warming of the polar stratosphere is as strong as in winter 3 but

https://doi.org/10.5194/egusphere-2024-1302
Preprint. Discussion started: 21 May 2024

more spread out into midlatitudes. This response in winter 2 does not lead to as many SSWs despite the weaker zonal winds, but it does appear to act as an important precursor to the significant increase in SSWs detected in winter 3. As for the second winter, the zonal wind weakening is still asymmetric and confined over the pole so this weakening is also not identified in the U50 index of Fig. 3c.

Furthermore, almost no downward stratospheric wave activity flux (Supplementary Fig. S1c) is detected in winter 3 where the upward flux is mostly circumpolar between 40° and 60° N, agreeing with the detected SSW response.

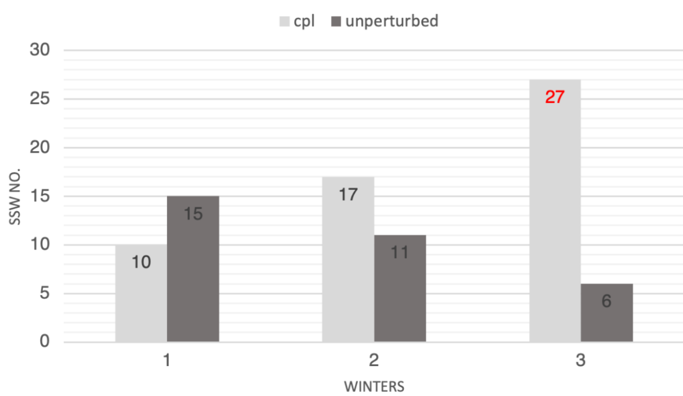

Figure 5: The sum of all SSW events in each experiment (all 20 ensemble members) of winters 1-3 both for *cpl* (light-gray bars) and control (dark bars). The color red indicates 95% significance according to a two-sided student's t test.

3.2.4. Winters 1-2 in *atm-only*: a comparison to *cpl*

The *atm-only* experiment provides valuable information to understand the mechanisms behind the response detected in the *cpl* experiment. Winter 1 in *atm-only* shows a similar thermal wind mechanism at play as for the *cpl* experiment (Fig. 6a and 4a, respectively). However, a stark difference between *cpl* and *atm-only* is detected in winter 2 when anomalous patterns in *cpl* (Fig. 4b) reveal a different mechanism occurring within the coupled climate system compared to the standalone atmosphere as shown in Fig. 6b. While *atm-only* exhibits in winter 2 a response similar to winter 1, a significant warming emerges in *cpl* in winter 2 in the T50 over the polar stratosphere, along with a weakening of U50 (Fig. 4b). This difference is also detected

https://doi.org/10.5194/egusphere-2024-1302
Preprint. Discussion started: 21 May 2024

in the EP flux, with a strong increase in upward EP flux in the *cpl* winter 2 (Fig. 4e) protruding further up into the stratosphere compared to *atm-only* (Fig. 6d), demonstrating how dominating the stratospheric thermal response is in *atm-only*. We mainly see regions of downward Plumb flux at 850 hPa in winters 1-2 (Fig. 6e and 6f) with the exception of an upward Plumb flux over Greenland in winter 1 and Northern North Pacific and the Tibetian plateau in winter 2, most likely originating in orography.

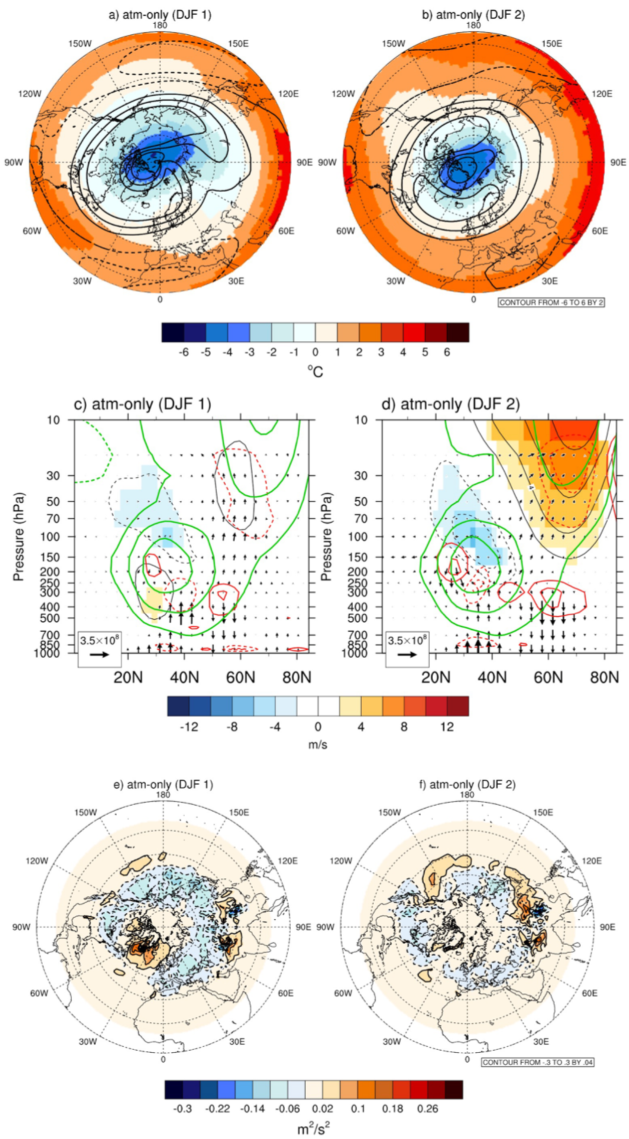

Figure 6: For the *atm-only* experiment. a-b) Zonal wind (contours) and temperature (shading) response at 50 hPa for winter 1 and winter 2, respectively. c-d) EP flux (arrows) and divergence (red contours) response along with zonal-mean zonal wind (black contours) and climatology (green contours, 2m) in winters 1-2, respectively. e-f) Vertical wave-activity (Plumb) flux anomalies at 850 hPa for winters 1-2, respectively. Contours and colored area indicate 95% significance according to a student's t-test.

3.3. The tropospheric response in *cpl*

In this section we present results from the first three winters of the *cpl* experiment to assess the surface imprint of the stratospheric anomalies detected following our idealized volcanic eruption and their potential impact on weather and surface climate in the Northern Hemisphere. In Fig. 7 the time evolution of the zonally averaged SST response is shown during the first 3 post-volcanic years. The strongest surface cooling takes place in midlatitudes during the second post-eruption summer.

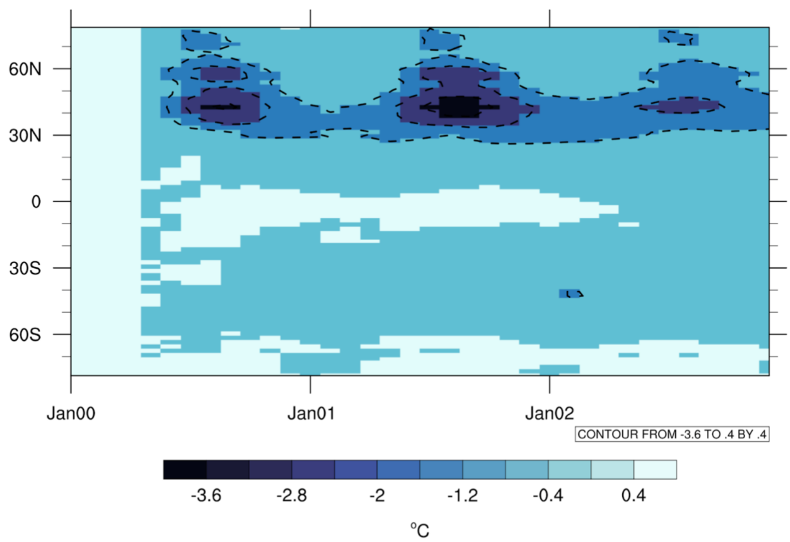

Figure 7: Time evolution of the zonally averaged SST response in the *cpl* experiment during the first three post-eruption years. Contours indicate 95% significance according to a two-tailed student's t-test.

https://doi.org/10.5194/egusphere-2024-1302
Preprint. Discussion started: 21 May 2024

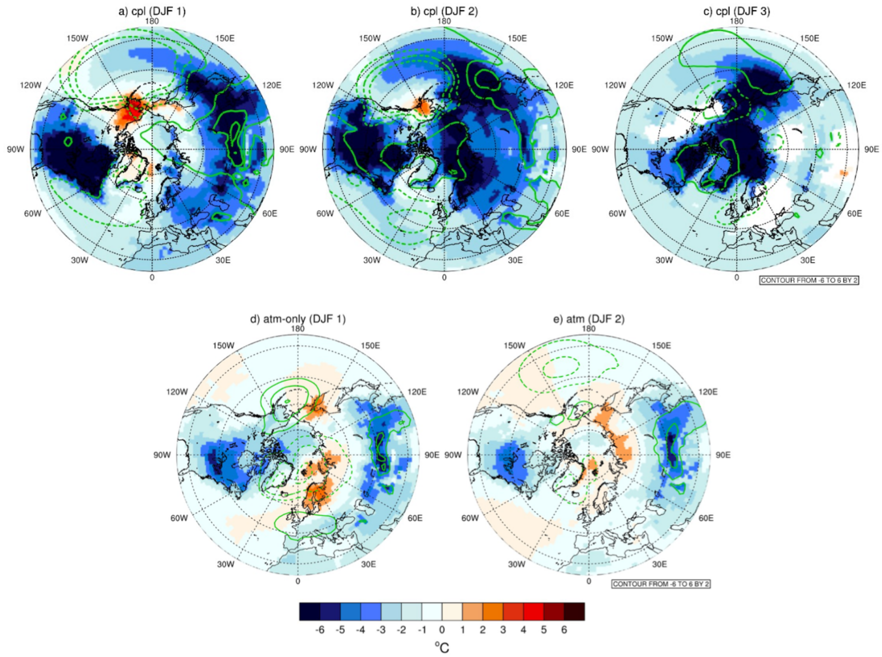

Figure 8: a-c) Sea level pressure (contours) and surface temperature (colored area) response in *cpl*, for winter 1-3, respectively. d-e) The same but for *atm-only* and winters 1-2, respectively. Contours and shaded areas indicate significance at the 95% confidence interval according to a student's t-test.

In Figure 8, the near-surface air temperature (T2m) and sea-level pressure (SLP) response is depicted for winter 1-3 in *cpl* and winters 1-2 in *atm-only,* for comparison. There is cooling of the midlatitude continents in *cpl* that is most pronounced over Siberia and eastern North America in winter 1 (Fig. 8a). The area of cooling increases in winter 2 when it emerges at higher latitudes before decreasing and becoming more confined to the higher latitudes in winter 3 (Fig. 8b-c). Meanwhile a slight significant warming is detected in winter 1 in the North Pacific, and NE and NW of Greenland (Fig. 8a). The surface cooling dominating the NH during winter 3 (Fig. 8c) occurs during the significant increase in SSWs also detected in winter 3 (Fig. 5), and this is a temperature pattern expected during such events. A different temperature response is detected in *atm-only* in winter 1 where a warming is present over N-Eurasia while cooling occurs over northern North America and the midlatitudes of Eurasia (Fig. 8d). In winter

https://doi.org/10.5194/egusphere-2024-1302
Preprint. Discussion started: 21 May 2024

2, the cooling is confined to the midlatitudes only, while the warming is located north of 60° N (Fig. 8e).

4 Summarizing discussions

Our two sets of atmosphere-only and coupled ocean-atmosphere experiments examine the large-scale climate response to an idealized long-lasting NH eruption. We assessed the first three winters of the *cpl* experiment and used the first two winters of *atm-only* as a comparison to investigate the dynamics that govern the stratospheric polar vortex and the associated surface response. Results from our *cpl* experiment show a similar response in the first winter as *atm-only*, with a strengthening of the zonal winds resulting from an aerosol-induced sharp temperature gradient between the midlatitudes and the pole (Fig. 4a). A distinct change to this pattern emerges in winter 2 where we detect an SSW-like pattern, with strong negative anomalies emerging in the polar U50 winds and a warming in the T50 field (Fig. 4b). This T50 warming is still present in winter 3 and coincides with an unexpected and significant increase in the number of SSW events (Fig. 4c and Fig. 5). The EP and Plumb fluxes (Fig. 4d-i) give further information on the source of this detected SSW increase where two mechanisms appears to be competing in the first three winters: a) A surface mechanism with strong upward wave activity flux and b) a stratospheric mechanism, where the strengthening of the U50 winds is due to a local heating by volcanic aerosols. The strength of each one determines which mechanism dominates in these three winters and hence the associated climate response.
In the first winter, the thermal forcing is stronger than the upward wave flux because of the large amount of aerosols present, thereby dominating the response. In the second winter, the thermal forcing from the volcanic aerosols at midlatitudes has decreased, allowing the strong upward wave flux to dominate and enter the upper stratosphere to weaken the zonal stratospheric winds (Fig. 5b and Fig. 4b). This upward wave flux and the weaker winds continue into winter 3, allowing for more frequent SSWs to develop (Fig. 4c and Fig. 5c, respectively), where the U50 weakening in winter 2 potentially plays a contributing role to the significant number of SSWs detected.

In our *atm-only* experiment the stratospheric warming by volcanic aerosols dominates the atmospheric circulation response in the first two post-eruption winters. Between June and September of the first two simulated years (not shown), strong radiative warming from the volcanic aerosols is present in the stratosphere between 30 and 60° N around the 50 hPa region.

https://doi.org/10.5194/egusphere-2024-1302
Preprint. Discussion started: 21 May 2024

In the following winters (winter 1 and 2), lack of solar radiation north of 60° N results in a strong temperature difference between the poles and midlatitudes (where sunlight is still a dominating factor) that leads to stronger stratospheric zonal winds and a stronger stratospheric polar vortex according to thermal wind balance and this isolates the cold air over the polar regions (Fig. 6a-b). The weaker westerlies in the midlatitudes occur due to the same mechanism but with a decrease in the meridional T gradient between equator and midlatitudes. This dominating stratospheric mechanism becomes clear as the EP flux diagnostics indicate little upward wave flux at 30-40° N compared to a stronger downward wave flux occurring at around 60° N. This purely atmospheric response following our idealized volcanic eruption is thus according to the standard theory following equatorial eruptions. This indicates that the stratospheric aerosol warming in WACCM4 is insensitive to the injection latitude in terms of the polar vortex response to volcanic eruptions since warming from both high- and mid-latitude eruptions will be confined to the midlatitudes during winter and warming from low latitude eruptions will be confined at low latitudes, both of which will increase the temperature gradient and trigger polar vortex strengthening.

As emphasized above, the difference between *cpl* and *atm-only* experiments gives valuable insight into the volcanically forced mechanisms at play within the coupled climate system in CESM1, where the short-term atmospheric response in our *cpl* experiment seems to depend more on the dynamic surface response than on the changes in stratospheric temperature gradients.

The strong surface cooling detected in Fig. 7 and 8 is a well-known caveat in the CMIP5 models (including CESM1) (Driscoll et al., 2012; Chylek et al., 2020) and is clearly detected in our coupled simulation. Furthermore, the stratospheric aerosol warming appears to be exaggerated in *atm-only* when compared to T50 fields from the coupled simulation while the strong surface cooling is absent. In other words, *atm-only* (WACCM4) exaggerates stratospheric warming of volcanic aerosols while the coupled version exaggerates volcanic surface cooling.
This exaggeration could also be attributed to the volcanic forcing being zonally symmetric and thus nearly homogeneously spread throughout the higher northern latitudes during peak forcing. However, the volcanic forcing is the same in *atm-only* and coupled experiments suggesting an intrinsic reason originating in the model itself. When the idealized volcanic forcing profile is compared to the other profiles used for scaling (Fig. 1), with the aerosol

https://doi.org/10.5194/egusphere-2024-1302
Preprint. Discussion started: 21 May 2024

lifetime being around 36 months for all curves, we would not expect drastic changes using a shorter eruption of similar injection size.

Although we do not focus specifically on the QBO, it is undeniably a dominating variability within the equatorial stratosphere that can influence the polar vortex differently depending on the state of the QBO. Each QBO cycle spans around 28 months on average but the number of ensemble members we have is only 20 and so we do not capture a complete QBO cycle in our *cpl* experiment. The potential impact this could have on our results was tested and from that it is clear that our *cpl* experiment is biased towards the easterly phase, where it is present in 14 ensemble members prior to the onset of our idealized volcanic eruption compared to the first 6 ensemble members having the westerly phase. The easterly phase of the QBO can impact the polar vortex by weakening it (Labe et al., 2019), thus allowing SSW events to develop more easily. To test the robustness of our results and the detected SSW in winter 3 with respect to the QBO, we also compared the ensemble members showing easterly phase with the westerly ones to test if the U50 and T50 response patterns would be different. They were not, both phases showed a weakening of the U50 although the zonal winds were more confined and consistent over the higher latitudes of the NH during the easterly phase (not shown). The difference in the number of ensemble members used for these calculations could of course impact the statistics of this test of ours but not the overall pattern detected. These results call for further studies on the relationship between NH eruptions and deterministic responses like SSWs, using both sensitivity experiments as well as observational datasets. Currently, work is ongoing to test the sensitivity of the polar vortex and the emerging SSWs to NH eruptions of smaller size as well as the long-term climate impacts. Establishing a link between NH eruptions and SSWs could serve as an important contribution in the improvement of decadal predictability of NH climate.

Data availability

The model output is available upon request by contacting the corresponding author.

Author contribution

HG conceptualized this study along with GM, YP and DZ. Cpl and atm-only experiments were carried out by HG and YP. Analysis and calculations of model output as well as graphical representation was done by HG. Manuscript draft was done by HG and editing was done by YP and DZ. GM served as the principal investigator of this work and did the final editing.

https://doi.org/10.5194/egusphere-2024-1302
Preprint. Discussion started: 21 May 2024

Competing interests

The corresponding author declares that none of the authors have any competing interest.

Acknowledgement

This work is supported by the Icelandic Research Fund (IRF), grant No. 2008-0445. HG is thankful to the Fulbright Scholar Program, which is sponsored by the U.S. department of state and Fulbright Iceland, that facilitated the stay of HG and her family in Irvine, CA during this work. We acknowledge high-performance computing support from Cheyenne (doi:10.5065/D6RX99HX) provided by NCAR's Computational and Information Systems Laboratory, sponsored by the National Science Foundation that we used for our experiments. HG also wants to thank the staff at the department of Earth System Science at UCI for the facility and assistance during this work and my stay at UCI. Finally, we want to thank Matthew Toohey for his assistance in the interpolation of the forcing files for WACCM4.

https://doi.org/10.5194/egusphere-2024-1302
Preprint. Discussion started: 21 May 2024

References

Azoulay, A., Schmidt, H., & Timmreck, C. (2021). The Arctic polar vortex response to volcanic forcing of different strengths. *Journal of Geophysical Research: Atmospheres*, *126*(11), e2020JD034450.

Baldwin, M. P., & Dunkerton, T. J. (1999). Propagation of the Arctic Oscillation from the stratosphere to the troposphere. *Journal of Geophysical Research: Atmospheres*, *104*(D24), 30937-30946.

Barsotti, S., Di Rienzo, D. I., Thordarson, T., Björnsson, B. B., & Karlsdóttir, S. (2018). Assessing impact to infrastructures due to tephra fallout from Öræfajökull volcano (Iceland) by using a scenario-based approach and a numerical model. *Frontiers in Earth Science*, *6*, 196.

Bittner M, Schmidt H, Timmreck C, Sienz F. Using a large ensemble of simulations to assess the Northern Hemisphere stratospheric dynamical response to tropical volcanic eruptions and its uncertainty. *Geophys Res Lett*. 2016;43(17):9324–32.

Brugnatelli, V., & Tibaldi, A. (2020). Effects in North Africa of the 934–940 CE Eldgjá and 1783–1784 CE Laki eruptions (Iceland) revealed by previously unrecognized written sources. *Bulletin of Volcanology*, *82*(11), 73.

Brown, F., Marshall, L., Haynes, P. H., Garcia, R. R., Birner, T., & Schmidt, A. (2023). On the magnitude and sensitivity of the quasi-biennial oscillation response to a tropical volcanic eruption. *Atmospheric Chemistry and Physics*, *23*(9), 5335-5353.

Charlton, A. J., & Polvani, L. M. (2007). A new look at stratospheric sudden warmings. Part I: Climatology and modeling benchmarks. *Journal of climate*, *20*(3), 449-469.

Church, J.A., White, N.J., Arblaster, J.M., 2005. Significant decadal-scale impact of volcanic eruptions on sea level and ocean heat content. *Nature* 438 (7064), 74–77.

Chylek, P., Folland, C., Klett, J. D., & Dubey, M. K. (2020). CMIP5 climate models overestimate cooling by volcanic aerosols. *Geophysical Research Letters*, *47*(3), e2020GL087047.

https://doi.org/10.5194/egusphere-2024-1302
Preprint. Discussion started: 21 May 2024

Colose CM, LeGrande AN, Vuille M. Hemispherically asymmetric volcanic forcing of tropical hydroclimate during the last millennium. *Earth Sys Dyn*. 2016;7(3):681–96. doi:10.5194/esd-7-681-2016.

DallaSanta, K., C. Orbe, D. Rind, L. Nazarenko, and J. Jonas. "Response of the Quasi-Biennial Oscillation to historical volcanic eruptions." *Geophysical Research Letters* 48, no. 20 (2021): e2021GL095412.

DallaSanta, K., & Polvani, L. M. (2022). Volcanic stratospheric injections up to 160 Tg (S) yield a Eurasian winter warming indistinguishable from internal variability. *Atmospheric Chemistry and Physics*, *22*(13), 8843-8862.

Dee, S. G., Cobb, K. M., Emile-Geay, J., Ault, T. R., Edwards, R. L., Cheng, H., & Charles, C. D. (2020). No consistent ENSO response to volcanic forcing over the last millennium. *Science*, *367*(6485), 1477-1481.

Domeisen, D. I., Grams, C. M., & Papritz, L. (2020). The role of North Atlantic–European weather regimes in the surface impact of sudden stratospheric warming events. *Weather and Climate Dynamics*, *1*(2), 373-388.

Driscoll, S., Bozzo, A., Gray, L. J., Robock, A., Stenchikov, G., 2012. Coupled ModelIntercomparison Project 5 (CMIP5) simulations of climate following volcanic erup-tions. *J. Geophys. Res.: Atmospheres,* 117 (D17).

Edmon, H.J., Hoskins, B.J. and McIntyre, M.E. (1980) Eliassen-Palm cross sections for the troposphere. *Journal of the Atmospheric Sciences*, **37**, 2600–2616.

Einarsson, P. (2019). Historical accounts of pre-eruption seismicity of Katla, Hekla, Öræfajökull and other volcanoes in Iceland. *Jökull*, *69*, 35-52.

Elsbury, D., Y. Peings and G. Magnusdottir, 2021. Variation in the Holton-Tan effect by longitude. Quarterly Journal of the Royal Meteorological Society. DOI: 10.1002/qj.3993

https://doi.org/10.5194/egusphere-2024-1302
Preprint. Discussion started: 21 May 2024

Fischer, H., Siggaard-Andersen, M.L., Ruth, U., Röthlisberger, R., Wolff, E., 2007. Glacial/interglacial changes in mineral dust and sea-salt records in polar ice cores: Sources,transport, and deposition. *Rev. Geophys*. (1), 45.

Gettelman, A., Schmidt, A., & Egill Kristjánsson, J. (2015). Icelandic volcanic emissions and climate. *Nature Geoscience*, *8*(4), 243-243.

Gleckler, P.J., AchutaRao, K., Gregory, J.M., Santer, B.D., Taylor, K.E., Wigley, T.M.L.,2006. Krakatoa lives: The effect of volcanic eruptions on ocean heat content and thermal expansion. Geophys. Res. Lett. (17), 33.

Graf, H.F., Perlwitz, J., Kirchner, I., 1994. Northern hemisphere tropospheric midlatitude circulation after violent volcanic eruptions. Contr. Atmos. Physics 67 (1), 3–13

Graf, H. F., Li, Q., & Giorgetta, M. A. (2007). Volcanic effects on climate: revisiting the mechanisms. *Atmospheric Chemistry and Physics*, *7*(17), 4503-4511.

Graf, H.-F., D. Zanchettin, C. Timmreck and M. Bittner (2014) Observational constraints on the tropospheric and near-surface winter signature of the Northern Hemisphere stratospheric polar vortex. Clim. Dyn., 43: 3245, doi:10.1007/s00382-014-2101-0

Guðlaugsdóttir, H., Steen-Larsen, H. C., Sjolte, J., Masson-Delmotte, V., Werner, M., & Sveinbjörnsdóttir, Á. E. (2018). The influence of volcanic eruptions on weather regimes over the North Atlantic simulated by ECHAM5/MPI-OM ensemble runs from 800 to 2000 CE. *Atmospheric Research*, *213*, 211-223.

Guðlaugsdóttir, H., Sjolte, J., Sveinbjörnsdóttir, Á. E., Werner, M., & Steen-Larsen, H. C. (2019). North Atlantic weather regimes in δ18O of winter precipitation: isotopic fingerprint of the response in the atmospheric circulation after volcanic eruptions. *Tellus B: Chemical and Physical Meteorology*, *71*(1), 1633848.

Haynes, P. H. (2005). Stratospheric dynamics. *Ann. Rev. Fluid Mech. doi: 10.1146/annurev.fluid.37.061903.175710*

https://doi.org/10.5194/egusphere-2024-1302
Preprint. Discussion started: 21 May 2024

Huang, J., Hitchcock, P., Maycock, A. C., McKenna, C. M., & Tian, W. (2021). Northern hemisphere cold air outbreaks are more likely to be severe during weak polar vortex conditions. *Communications Earth & Environment*, *2*(1), 147.

Hurrell, J.W., 1995. Decadal trends in the north atlantic oscillation: regional tempera-tures and precipitation. Science 269 (5224), 676–679.

Hurrell, J. W., Holland, M. M., Gent, P. R., Ghan, S., Kay, J. E., Kushner, P. J., ... & Marshall, S. (2013). The community earth system model: a framework for collaborative research. *Bulletin of the American Meteorological Society*, *94*(9), 1339-1360.

Jungclaus, J. H., Bard, E., Baroni, M., Braconnot, P., Cao, J., Chini, L. P., Egorova, T., Evans, M., González-Rouco, J. F., Goosse, H., Hurtt, G. C., Joos, F., Kaplan, J. O., Khodri, M., Klein Goldewijk, K., Krivova, N., LeGrande, A. N., Lorenz, S. J., Luterbacher, J., Man, W., Maycock, A. C., Meinshausen, M., Moberg, A., Muscheler, R., Nehrbass-Ahles, C., Otto-Bliesner, B. I., Phipps, S. J., Pongratz, J., Rozanov, E., Schmidt, G. A., Schmidt, H., Schmutz, W., Schurer, A., Shapiro, A. I., Sigl, M., Smerdon, J. E., Solanki, S. K., Timmreck, C., Toohey, M., Usoskin, I. G., Wagner, S., Wu, C.-J., Yeo, K. L., Zanchettin, D., Zhang, Q., and Zorita, E.: The PMIP4 contribution to CMIP6 – Part 3: The last millennium, scientific objective, and experimental design for the PMIP4 past1000 simulations, Geosci. Model Dev., 10, 4005-4033, https://doi.org/10.5194/gmd-10-4005-2017, 2017

Khodri, M., Izumo, T., Vialard, J., Janicot, S., Cassou, C., Lengaigne, M., et al. (2017). Tropical explosive volcanic eruptions can trigger El Niño by cooling tropical Africa. Nature Communications, 8(1), 778. https://doi.org/10.1038/s41467-017-00755-6

Kim, B.M., Son, S.W., Min, S.K., Jeong, J.H., Kim, S.J., Zhang, X., Shim, T., Yoon, J.H.,2014. Weakening of the stratospheric polar vortex by arctic sea-ice loss. Nat.Commun. 5, 4646.

Kodera, K., 1994. Influence of volcanic eruptions on the troposphere through strato-spheric dynamical processes in the northern hemisphere winter. J. Geophys. Res.-Atmos. 99 (D1), 1273–1282

https://doi.org/10.5194/egusphere-2024-1302
Preprint. Discussion started: 21 May 2024

Kolstad, E. W., Lee, S. H., Butler, A. H., Domeisen, D. I., & Wulff, C. O. (2022). Diverse surface signatures of stratospheric polar vortex anomalies. *Journal of Geophysical Research: Atmospheres*, *127*(20), e2022JD037422.

Labe, Z., Peings, Y., & Magnusdottir, G. (2019). The effect of QBO phase on the atmospheric response to projected Arctic sea ice loss in early winter. *Geophysical Research Letters*, *46*(13), 7663-7671.

Larsen, G., & Gudmundsson, M. T. (2014). Volcanic system: Bárðarbunga system. *Catalogue of Icelandic Volcanoes*, 1-11.

Lehtonen, I., & Karpechko, A. Y. (2016). Observed and modeled tropospheric cold anomalies associated with sudden stratospheric warmings. *Journal of Geophysical Research: Atmospheres*, *121*(4), 1591-1610.

Marsh, Daniel R., Michael J. Mills, Douglas E. Kinnison, Jean-Francois Lamarque, Natalia Calvo, and Lorenzo M. Polvani. "Climate change from 1850 to 2005 simulated in CESM1 (WACCM)." *Journal of climate* 26, no. 19 (2013): 7372-7391.

Neely III, R. R., Conley, A. J., Vitt, F., & Lamarque, J. F. (2016). A consistent prescription of stratospheric aerosol for both radiation and chemistry in the Community Earth System Model (CESM1). *Geoscientific Model Development*, *9*(7), 2459-2470.

Omrani, N.-E., Keenlyside, N., Matthes, K., Boljka, L., Zanchettin, D., Jungclaus, J. H., Lubis, S. W. (2022) Coupled stratosphere-troposphere-Atlantic multidecadal oscillation and its importance for near-future climate projection. npj Climate and Atmospheric Science, 5, 59, https://doi.org/10.1038/s41612-022-00275-1

Oppenheimer, C., Orchard, A., Stoffel, M., Newfield, T. P., Guillet, S., Corona, C., ... & Büntgen, U. (2018). The Eldgjá eruption: timing, long-range impacts and influence on the Christianisation of Iceland. *Climatic Change*, *147*, 369-381.Otterå, O.H., Bentsen, M., Drange, H., Suo, L., 2010. External forcing as a metronome foratlantic multidecadal variability. Nat. Geosci. 3 (10), 688–694

Ortega, P., Swingedouw, D., Masson-Delmotte, V., Risi, C., Vinther, B., Yiou, P., Vautard,R., Yoshimura, K., 2014. Characterizing atmospheric circulation signals in.

https://doi.org/10.5194/egusphere-2024-1302
Preprint. Discussion started: 21 May 2024

Greenlandice cores: insights from a weather regime approach. Clim. Dyn. 43 (9–10),2585–2605

Otterå, O. H., Bentsen, M., Drange, H., & Suo, L. (2010). External forcing as a metronome for Atlantic multidecadal variability. *Nature Geoscience*, *3*(10), 688-694.

Pausata, F. S. R., Chafik, L., Caballero, R. & Battisti, D. S. Impacts of high- latitude volcanic eruptions on ENSO and AMOC. Proc. Natl Acad. Sci. 112, 13784–13788 (2015).

Pausata, F.S.R., D. Zanchettin, C. Karamperidou, R. Caballero, and D. S. Battisti (2020) ITCZ shift and extratropical teleconnections drive ENSO response to volcanic eruptions. Science Advances 6(23) eaaz5006, doi: 10.1126/sciadv.aaz5006

Pausata, F. S. R., Zhao, Y., Zanchettin, D., Caballero, R., & Battisti, D. S. (2023). Revisiting the mechanisms of ENSO response to tropical volcanic eruptions. Geophysical Research Letters, 50, e2022GL102183. https://doi.org/10.1029/2022GL102183

Perlwitz, J., Graf, H.F., 1995. The statistical connection between tropospheric and. stra-tospheric circulation of the Northern Hemisphere in winter. J. Clim. (10),2281–2295

Peings, Y., & Magnusdottir, G. (2014). Response of the wintertime Northern Hemisphere atmospheric circulation to current and projected Arctic sea ice decline: A numerical study with CAM5. *Journal of Climate*, *27*(1), 244-264.

Plumb, R. A. (1985). On the three-dimensional propagation of stationary waves. *Journal of Atmospheric Sciences*, *42*(3), 217-229.

Polvani, L. M., Banerjee, A., & Schmidt, A. (2019). Northern Hemisphere continental winter warming following the 1991 Mt. Pinatubo eruption: reconciling models and observations. *Atmospheric Chemistry and Physics*, *19*(9), 6351-6366.

Predybaylo, E., Stenchikov, G., Wittenberg, A. T. & Osipov, S. El Niño/ Southern Oscillation response to low-latitude volcanic eruptions depends on ocean pre-conditions and eruption timing. Commun. Earth Environ. 1, 1–13 (2020).

Rayner, N. A. A., Parker, D. E., Horton, E. B., Folland, C. K., Alexander, L. V., Rowell, D. P., ... & Kaplan, A. (2003). Global analyses of sea surface temperature, sea ice, and night

https://doi.org/10.5194/egusphere-2024-1302
Preprint. Discussion started: 21 May 2024

marine air temperature since the late nineteenth century. *Journal of Geophysical Research: Atmospheres*, *108*(D14).

Robock, A., Mao, J., 1992. Winter warming from large volcanic eruptions. Geophys. Res.Lett. 19 (24), 2405–2408.

Robock, A., 2000. Volcanic eruptions and climate. Rev. Geophys. 38 (2), 191–219.

Screen, J. A., Deser, C., Smith, D. M., Zhang, X., Blackport, R., Kushner, P. J., ... & Sun, L. (2018). Consistency and discrepancy in the atmospheric response to Arctic sea-ice loss across climate models. *Nature Geoscience*, *11*(3), 155-163.

Shindell, D.T., Schmidt, G.A., Mann, M.E., Faluvegi, G., 2009. Dynamic winter. Climate response to large tropical volcanic eruptions since 1600. J. Geophys. Res.-Atmos.(D5), 109.Sigl, M., Winstrup, M., McConnell, J.R., Welten, K.C., Plunkett, G., Ludlow, F., Buntgen,U., Caffee, M., Chellman, N., Dahl-Jensen, D., Fischer, H., 2009. Timing and climate forcing of volcanic eruptions for the past 2500 years. Nature 523 (7562), 543–549

Sjolte, J., Adolphi, F., Guðlaugsdòttir, H., & Muscheler, R. (2021). Major Differences in Regional Climate Impact Between High-and Low-Latitude Volcanic Eruptions. *Geophysical Research Letters*, *48*(8), e2020GL092017.

Smith, K. L., Neely, R. R., Marsh, D. R., & Polvani, L. M. (2014). The specified chemistry whole atmosphere community climate model (SC-WACCM). *Journal of Advances in Modeling Earth Systems*, *6*(3), 883-901.

Stenchikov, G., Robock, A., Ramaswamy, V., Schwarzkopf, M.D., Hamilton, K.,Ramachandran, S., 2002. Arctic Oscillation response to the 1991 Mount Pinatubo.eruption: Effects of volcanic aerosols and ozone depletion. J. Geophys. Res.-Atmos.(D24), 107.

Stenchikov, G., Delworth, T.L., Ramaswamy, V., Stouffer, R.J., Wittenberg, A., Zeng, F.,2009. Volcanic signals in oceans. J. Geophys. Res.-Atmos. (D16), 114.

Stothers, R. B. (1998). Far reach of the tenth century Eldgjá eruption, Iceland. *Climatic Change*, *39*(4), 715-726.

https://doi.org/10.5194/egusphere-2024-1302
Preprint. Discussion started: 21 May 2024

Swingedouw, D., Ortega, P., Mignot, J., Guilyardi, E., Masson-Delmotte, V., Butler, P.G.,Khodri, M., Séférian, R., 2015. Bidecadal North Atlantic ocean circulation variability controlled by timing of volcanic eruptions. Nat. Commun. 6, 6545.

Thomas, M. A., Giorgetta, M. A., Timmreck, C., Graf, H. F., & Stenchikov, G. (2009). Simulation of the climate impact of Mt. Pinatubo eruption using ECHAM5–Part 2: Sensitivity to the phase of the QBO and ENSO. *Atmospheric Chemistry and Physics*, *9*(9), 3001-3009.

Timmreck, C.: Modeling the climatic effects of large explosive volcanic eruptions, Wiley Interdisciplinary Reviews: Climate Change, 3, 545–564, 2012.

Toohey, M., Krüger, K., Bittner, M., Timmreck, C., and Schmidt, H.: The impact of volcanic aerosol on the Northern Hemisphere stratospheric polar vortex: mechanisms and sensitivity to forcing structure, Atmos. Chem. Phys., 14, 13063–13079, https://doi.org/10.5194/acp-14-13063-2014, 2014.

Zambri, B., Robock, A., Mills, M. J., & Schmidt, A. (2019). Modeling the 1783–1784 Laki eruption in Iceland: 2. Climate impacts. *Journal of Geophysical Research: Atmospheres*, *124*(13), 6770-6790.

Zanchettin, D., Timmreck, C., Graf, H.F., Rubino, A., Lorenz, S., Lohmann, K., Jungclaus,J.H., 2012. Bi-decadal variability excited in the coupled ocean-atmosphere system by strong tropical volcanic eruptions. Clim. Dyn. 39 (1–2), 419–444.

Zanchettin, D., Timmreck, C., Bothe, O., Lorenz, S.J., Hegerl, G., Graf, H.F., Lutherbacher,J., Jungclaus, J.H., 2013. Delayed winter warming: A robust decadal response to strong tropical volcanic eruptions. Geophys. Res. Lett. 40 (1), 204–209.

Zanchettin, D., Khodri, M., Timmreck, C., Toohey, M., Schmidt, A., Gerber, E. P., Hegerl, G., Robock, A., Pausata, F. S. R., Ball, W. T., Bauer, S. E., Bekki, S., Dhomse, S. S., LeGrande, A. N., Mann, G. W., Marshall, L., Mills, M., Marchand, M., Niemeier, U., Poulain, V., Rozanov, E., Rubino, A., Stenke, A., Tsigaridis, K., and Tummon, F.: The Model Intercomparison Project on the climatic response to Volcanic forcing (VolMIP): experimental design and forcing input data for CMIP6, Geosci. Model Dev., 9, 2701-2719, doi:10.5194/gmd-9-2701-2016, 2016.

https://doi.org/10.5194/egusphere-2024-1302
Preprint. Discussion started: 21 May 2024

Zanchettin, D. (2017) Aerosol and Solar Irradiance Effects on Decadal Climate Variability and Predictability. Current Climate Change Reports, 3, 150, doi:10.1007/s40641-017-0065-y

Zanchettin, D., Timmreck, C., Khodri, M., Schmidt, A., Toohey, M., Abe, M., Bekki, S., Cole, J., Fang, S.-W., Feng, W., Hegerl, G., Johnson, B., Lebas, N., LeGrande, A. N., Mann, G. W., Marshall, L., Rieger, L., Robock, A., Rubinetti, S., Tsigaridis, K., and Weierbach, H.: Effects of forcing differences and initial conditions on inter-model agreement in the VolMIP volc-pinatubo-full experiment, Geosci. Model Dev., 15, 2265–2292, https://doi.org/10.5194/gmd-15-2265-2022, 2022

Zhu, F., Emile-Geay, J., Anchukaitis, K. J., Hakim, G. J., Wittenberg, A. T., Morales, M. S., ... & King, J. (2022). A re-appraisal of the ENSO response to volcanism with paleoclimate data assimilation. *Nature communications*, *13*(1), 747.

Thordarson, T., & Self, S. (2003). Atmospheric and environmental effects of the 1783–1784 Laki eruption: A review and reassessment. *Journal of Geophysical Research: Atmospheres*, *108*(D1), AAC-7.

Toohey, M., Krüger, K., Bittner, M., Timmreck, C., & Schmidt, H. (2014). The impact of volcanic aerosol on the Northern Hemisphere stratospheric polar vortex: mechanisms and sensitivity to forcing structure. *Atmospheric Chemistry and Physics*, *14*(23), 13063-13079.

Toohey, M., Stevens, B., Schmidt, H., & Timmreck, C. (2016). Easy Volcanic Aerosol (EVA v1. 0): an idealized forcing generator for climate simulations. *Geoscientific Model Development*, *9*(11), 4049-4070.

Weierbach, H., LeGrande, A. N., & Tsigaridis, K. (2023). The impact of ENSO and NAO initial conditions and anomalies on the modeled response to Pinatubo-sized volcanic forcing. *Atmospheric Chemistry and Physics*, *23*(24), 15491-15505.